ELSEVIER

Journal of Photochemistry and Photobiology A: Chemistry 119 (1998) 191–203

Journal of Photochemistry and Photobiology A:Chemistry

Complex formation between symmetrical thiacyanine dyes and aromatic heterocycles: evidence for molecular recognition

Amanda Coreen Bruce[a], Monica Chadha[a], Angela Farrah Marks[a], M.R.V. Sahyun[a,*], Susan E. Hill[b]

[a]*Department of Chemistry, University of Wisconsin – Eau Claire, Eau Claire, WI 54702, USA*
[b]*Imation Corp., Oakdale, MN 55128, USA*

Received 21 May 1998; received in revised form 20 July 1998; accepted 4 August 1998

Abstract

Complexes between three thiacarbocyanine dyes and imidazole, **Im**, benzimidazole, **Bz**, and 2-methylbenzimidazole, **2-MeBz**, have been detected by perturbation of the dyes' fluorescence. In some cases 1 : 2, as well as 1 : 1 complexes, can be observed. This assignment has been confirmed by time-resolved laser flash spectroscopy, detected by transient absorption spectroscopy. Based on a preconception of complex geometry, we selected a series of α,ω-bis(2-benzimidazolyl)alkanes of chain length n, as complexing agents which we anticipated might exhibit molecular recognition towards the cyanine chromophores. A modicum of molecular recognition was indeed observed when $(n-4)$ matched the number of carbon atoms in the polymethine chain of the dye. Computational chemical studies using the Merck molecular force field and AM1 semi-empirical molecular orbital calculation were carried out to elucidate complex structure. Geometry of the **Im** and **Bz** complexes turned out to be quite different. The calculated geometry of the latter complexes turned out to be incompatible with the anticipated basis for molecular recognition. The computational studies suggested the basis for dye-complexing agent interaction in the ground state to be principally electrostatic, i.e., with little or no dispersion or charge transfer contributions.

Keywords: Thiacyanine dyes; Aromatic heterocycles; Molecular recognition

1. Introduction

Recently we reported evidence that at least one cyanine dye forms ground state complexes with aromatic amines, but not with aliphatic amines of comparable ionization potential [1]. The complexes were experimentally detectable through quenching (and, in one case, enhancement) of the fluorescence of the 3,3′-diethyl-2,2′-thiacyanine cation. This result implies that the aromatic amine mediates excited state relaxation of the cyanine dye. Because the emissive lifetime of this cyanine cation is too short to allow dynamic encounter with potential quenchers in solution [1], we postulated ground-state complex formation to explain these results. Accordingly, mediation of radiationless deactivation of complexed dye may involve introduction of a new decay pathway, namely non-adiabatic thermalization of excitation energy into complex dissociation. Similar results have been reported recently for diazapyrene derivatives with adenine and adenosine [2].

We felt that these results in the cyanine dye system required further investigation to:

1. establish the generality of the phenomenon;
2. confirm its previous interpretation specifically as π-complex formation; and
3. explore its possible exploitation in a scheme for molecular recognition involving cyanine chromophores.

Complex formation may be related to the utility of certain cyanine dyes for DNA-labelling [3,4]. It should be noted that complexation of cyanine dyes to DNA strands leads, at the most, to very subtle changes in ground state absorption spectra [2,3]; at the same time large enhancements of dye fluorescence may result [3–6]. Quenching, when observed under these conditions, has been attributed to an electron transfer mechanism [3]; fluorescence enhancement has been attributed to restriction of the torsional relaxation of the excited state of the complexed dye, which decreases the rates of non-radiative relaxation pathways [7]. Torsional relaxation is usually cited as the principal pathway for

*Corresponding author. E-mail: sahyun@pioneerplanet.infi.net

1010-6030/98/$ – see front matter
PII: S1010-6030(98)00371-2

non-radiative decay of the S_1 state of cyanine chromophores [7–11], coupled, in part, to dye isomerization [8,12–14], and, also, to intersystem crossing [15,16]. For longer chain length dyes, e.g., tricarbocyanines, other modes may become important in non-radiative relaxation [16,17].

For this work we chose a homologous series of symmetrical 3,3′-diethyl-2,2′-thiacarbocyanine dyes, **I**, **II**, and **III**, with 3, 5 and 7 carbon atoms in the polymethine chain, respectively.

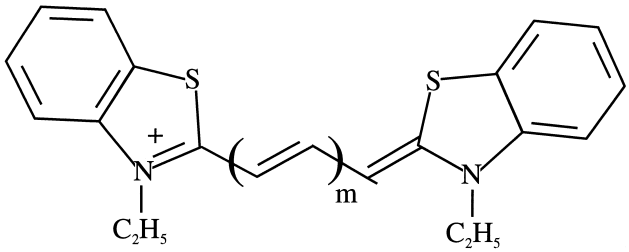

Dye I	m=1
Dye II	m=2
Dye III	m=3

The photophysics of these dyes in various solvents have been studied extensively [7,15,16]. As complexing agents we selected imidazole, benzimidazole, and 2-methylbenzimidazole. We expected strong π-overlap between the aromatic heterocycles of the cyanine chromophores and the complexing agents. At the same time, we also expected that with these molecules electron-transfer quenching could be excluded. Furthermore, differences in complexing activity between imidazole and benzimidazole should provide a test of our hypothesis that their interaction with the cyanine dyes represents π-complexation.

For the molecular recognition aspect of the work, we selected a series of symmetrical α,ω-bis(2-benzimidazolyl)-alkanes, with 3, 5, 7, 9, and 11 methylene carbons in the alkane chain as candidate complexing agents. These α,ω-bis(2-benzimidazolyl)alkanes are known compounds, of interest in their own right as antiviral and bactericidal agents [19,20], corrosion inhibitors [21], and as ligands for metal ion separation [22].

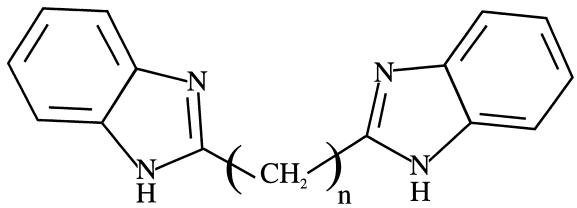

According to principles of self-organizing systems [18] we envisioned formation of sandwich-type π-complexes simultaneously at both ends of the cyanine chromophore, when the lengths of the polymethine chain in the dye and of the alkane chain in the complexing agent comprised the same number of carbon atoms. This proposal is shown in Scheme 1.

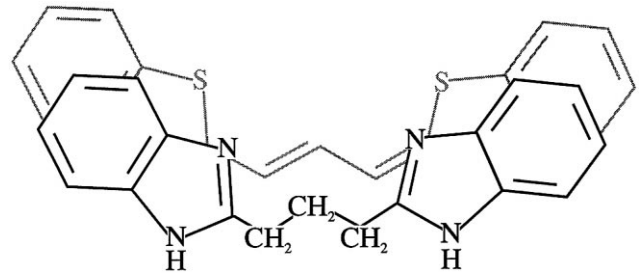

Scheme 1.

2. Experimental details

2.1. Materials

The following dyes were used as received from the vendors:

I: 3,3′-diethyl-2,2′-thiacarbocyanine iodide (H.W. Sands)
II: 3,3′-diethyl-2,2′-thiadicarbocyanine iodide (Eastman Kodak)
III: 3,3′-diethyl-2,2′-thiatricarbocyanine iodide (Pfaltz and Bauer)

All were subjected to thin layer chromatography (TLC) on Whatman (Whatman International, Maidstone, UK) type K5F silica gel plates using a series of methanol–methylene chloride mixtures as elution solvents. Only one coloured or fluorescent component could be detected in each case. With iodine development of the TLC plates, a trace amount of a very mobile, colourless, low molecular weight component could be detected in the case of dye **II**; traces of immobile (polymeric?) species, perhaps oxidation products of the dyes, could be detected in the cases of both dyes **II** and **III**. It was not expected that these materials would interfere in any way with the planned experiments. Photophysical measurements previously made on the same dye samples [16] were in good agreement with literature values.

Spectroscopic grade solvents, EM Omnisolv™ methanol, Aldrich 'spectrophotometric grade' 1-propanol, Spectro-Solv™ acetone and acetonitrile (Spectra Chemicals), were used for all fluorimetric and time-resolved experiments. Imidazole (Kodak), benzimidazole and 2-methylbenzimidazole (both Aldrich Chemicals, '99+ %') samples as received exhibited correct melting points and 400 MHz proton NMR spectra. They were accordingly used without further purification.

After evaluation of several preparative methods for obtaining the α,ω-bis(2-benzimidazolyl)alkanes, we found the method of Vas and co-workers [23] to be the most

satisfactory. All samples used in the present work were accordingly obtained by this method, which involves condensation of two moles of *o*-phenylenediamine (Aldrich) with the appropriate α,ω-alkane dicarboxylic acid in hot polyphosphoric acid. Compounds as prepared and purified exhibited melting points in agreement with the literature [23], as well as correct 400 MHz proton NMR spectra.

2.2. Methods

All compounds used in this study were analyzed electrochemically on a Bioanalytical Systems CV50 voltammetric analyzer operating in the Osteryoung square-wave voltammetric mode [24]. Analyses were carried out in (90/10) acetonitrile–methanol using 0.01 M tetrabutylammonium tetrafluoroborate (Aldrich) as supporting electrolyte. Cyanine dyes exhibited reversible one-electron peaks at potentials within ±0.03 V of the best available literature values [25]. In the cases of dyes **I** and **II**, the iodide counterion peak at +0.47 V (vs. Ag–AgBr) was clearly resolved, but it was convoluted with the dye redox peaks in the case of dye **III**. Complexing agents, imidazole, benzimidazole and the α,ω-bis(2-benzimidazolyl)alkanes, did not show any evidence of reversible electrochemistry within the window of the experiment (−0.7–+1.0 V vs. Ag–AgBr), consistent with our expectation that these materials would not undergo electron-transfer interaction with the dyes in either their ground or S_1 excited states.

Fluorimetric detection of complex formation was carried out on a Perkin-Elmer MPF44B spectrofluorimeter, operating in the 'ratio' mode. This instrument was modified by substitution of a Hamamatsu model 933 photomultiplier tube, in order to enhance signal-to-noise response of the instrument at long wavelengths. Fluorescence intensity was monitored at the wavelength of maximum emission of the dye, λ_{em}, excited by light of the wavelength corresponding to the dye's absorption maximum, λ_{ex}. Absorption and fluorescence spectra of these dyes in various solvents have been reported previously [7,15,16]. Fluorimetric titrations were carried out at room temperature as follows. Two (2.5 ml) aliquots of a solution 1×10^{-6} M of the cyanine dye in the appropriate solvent were placed into two matched quartz spectrofluorimeter cuvettes. To these were added a series of 100 μl aliquots of the solvent (control) and of the complexing agent, 0.1 M in the solvent (test), respectively. Readings were taken of each solution after each addition, and the intensities obtained from the control and test aliquots ratioed to give I_o/I for each increment of solvent and complexing agent. This approach obviated the need to provide additional correction for the non-trivial dilution of the sample on addition of the complexing agent solution.

Computational modelling of the molecules used in this study was carried out using the SPARTAN package [26–28]. In general a molecular mechanics geometry search using the Merck force field was carried out to find a minimum energy starting point for appropriate isomers of each compound. The SPARTAN algorithm allowed application of geometric constraints in order to estimate strain energy differences between the minimum energy conformation of a compound and other hypothesized conformations. From this point, a full AM1 (semi-empirical molecular orbital) geometry optimization could be carried out. An Osawa conformation search could then be carried out to re-evaluate the identification of geometries associated with strain energy minima.

Lifetimes of the S_1 states of the cyanine dyes in methanol solution were obtained by pump-probe laser flash spectroscopy as described previously [29], with 30 ps laser flash excitation at 532 nm. Correlation time (time resolution) for the measurements was ca. 25 ps. From these spectra the kinetics of recovery of the dye ground state could be monitored as in the previous [1,15,16] studies.

3. Results and discussion

3.1. Fluorimetric titration of dyes with complexing agents

Fluorimetric titration of dyes **I**, **II**, and **III** with imidazole, **Im**, benzimidazole, **Bz**, and 2-methylbenzimidazole, **2-MeBz**, was carried out in acetonitrile, acetone, 1-propanol, and methanol. In many cases quenching was observed where the quenching ratio, I_o/I, varied linearly with the concentration of complexing agent, [Q] (Q = **Im**, **Bz**, or **2-MeBz**), according to the Stern–Volmer form,

$$I_o/I = 1 + K_1[\mathrm{Q}] \quad (1)$$

where, typically, $1 \leq K_1 \leq 10\ \mathrm{M}^{-1}$. Signal-to-noise ratios under our experimental conditions precluded detection of $K_1 \leq 1\ \mathrm{M}^{-1}$. A representative Stern–Volmer plot for dye **I** with **Bz** in 1-propanol is shown in Fig. 1. Estimates of K_1 are given in Table 1. As in the previous study of complexation of 3,3′-diethyl-2,2′-thiacyanine, values of K_1 for dye **I**, whose fluorescence lifetime in methanol is ca. 0.1 ns, are nearly an order of magnitude too large for dynamic quench-

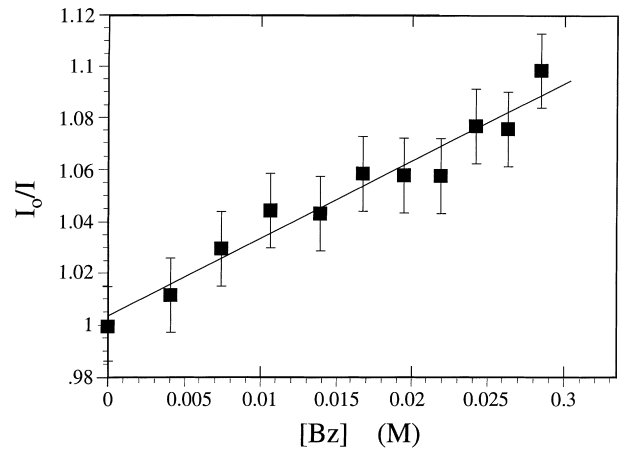

Fig. 1. Stern–Volmer plot for quenching of fluorescence of dye **I** by **Bz** in 1-propanol.

Table 1
Parameters for fluorescence quenching and/or enhancement: cyanine dyes **I**, **II** and **III** with imidazole (**Im**) and benzimidazole (**Bz**)

	Dye	K_1 (M^{-1})	K'' (M^{-2})	K_2 (M^{-2})
Im in methanol	**I**	(4.9 ± 1.7)	–[b]	–
	II	(5.3 ± 0.6)	(192 ± 75)	–
Bz in methanol	**I**	(9.1 ± 2.7)	(118 ± 10)	(20 ± 2.4)
	II	(6.7 ± 1.9)	(263 ± 75)	(130 ± 40)
2-MeBz in methanol	**II**	2.1	–[b]	–
	III	6.3	–[b]	–
Bz in acetonitrile	**I**	–[a]	–[b]	–
	II	(5.3 ± 1.8)	99	–
	III	(3 ± 1)	–[b]	–
Bz in 1-propanol	**I**	(2.5 ± 1.2)	–[b]	–
	II	–[a]	–[b]	–
2-MeBz in 1-propanol	**II**	–[a]	–[b]	–
	III	6.4	–[b]	–
Bz in acetone	**I**	(5.8 ± 0.75)[c]	–[b]	–
	II	3.7[c]	–[b]	–
	III	2.5[c]	–[b]	–
2-MeBz in acetone	**II**	–[a]	–[b]	–
	III	4.4	–[b]	–

[a] $K_1 \leq 1\ M^{-1}$.
[b] $K'' \leq 25\ M^{-2}$.
[c] Estimated from double reciprocal plot, e.g., Fig. 2.

ing; some ground state interaction between dye **I** and **Im** or **Bz** must accordingly be inferred. According to our hypothesis that this interaction is π-complex formation, K_1 is the association constant for the complex, provided the complex is fluorescence-inactive if there is appreciable fluorescence from the excited complex application of Eq. (1) tends to underestimate the value of the formation constant, characteristic deviation from linearity in the Stern–Volmer plot should be observed. We are inclined to the same interpretation of the K_1-values for dyes **II** and **III**, though in these cases diffusional interaction of the dyes with complexing agent cannot be excluded on the basis of the steady-state experiments.

In the case of dye **I** in acetone, complex formation appears to lead to fluorescence enhancement. Accordingly regression of the fluorescence intensity ratio on [Q] does not give the association constant directly. If where the fluorescence quantum efficiency of the dye is given by Φ_{dye} and that of the complex by $\Phi_{complex}$, the observed fluorescence quantum efficiency in the presence of [Q] is

$$\Phi_{obs} = \Phi_{dye}\left(1 - f_{complex}\right) + \Phi_{complex} f_{complex} \quad (2)$$

where $f_{complex}$ is the fraction of the dye concentration converted to the emissive complex. Since $f_{complex} = \{1 + (K_1[Q])^{-1}\}^{-1}$

$$\Phi_{obs}/\Phi_{dye} = 1 + \left[\left(\Phi_{complex}/\Phi_{dye}\right) - 1\right]\left\{1 + (K_1[Q])^{-1}\right\}^{-1} \quad (3)$$

i.e., using $I/I_o = \Phi_{obs}/\Phi_{dye}$, insofar as the spectral distribution of emission is unaltered on complexation.

$$(I/I_o - 1)^{-1} = \left[\left(\Phi_{complex}/\Phi_{dye}\right) - 1\right]^{-1} + \left\{\left[\left(\Phi_{complex}/\Phi_{dye}\right) - 1\right]K_1[Q]\right\}^{-1} \quad (4)$$

A 'double reciprocal' plot according to Eq. (4), for dye **I** with **Bz**, is shown in Fig. 2. The intercept in this case yields $\Phi_{complex}/\Phi_{dye} = 2.15$, and from the slope we estimate a value for $K_1 = (5.8 \pm 0.75)$ which is comparable to the estimates of the complex formation constant obtained under conditions of fluorescence quenching.

In still other cases, strongly non-linear dependence of fluorescence intensity on complexing agent concentration was observed. These data, as illustrated by the graph in Fig. 3 for dye **II** with **Bz** in methanol, were fit to an empirical quadratic equation

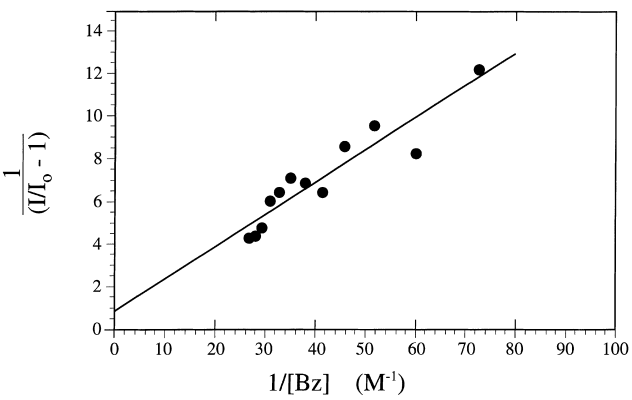

Fig. 2. Double reciprocal plot describing enhancement of fluorescence of dye **I** through complexation by **Bz** in acetone.

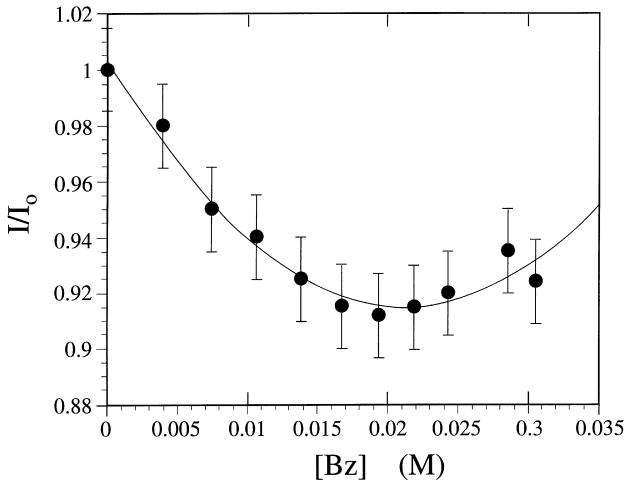

Fig. 3. Analysis of non-linear dependence of fluorescence intensity for dye **II** on concentration of added **Bz** in methanol according to Eq. (5).

$$I/I_o = K''[\mathrm{Q}]^2 - K_1[\mathrm{Q}] + 1 \quad (5)$$

for which a rationale is provided in the Appendix A. Accordingly, just as in Eq. (1), K_1 is the association constant for 1 : 1 complex formation, again assuming that the 1 : 1 complex is fluorescence-inactive. Then, from Eq. (A9) in the Appendix A, $K'' = (\Phi_{\mathrm{complex}}/\Phi_{\mathrm{dye}} - 1)K_2$, where K_2 is the formation constant for an emissive ternary complex (2 complexing agent : 1 dye) whose fluorescence quantum efficiency is Φ_{complex}. Values of K'' and K_1 obtained by this analysis are also given in Table 1. Reproducibility of these results and goodness-of-fit statistics suggested that where $K'' \leq 25\ \mathrm{M}^{-2}$, the quadratic fit could not be distinguished from a fit to Eq. (1). Again, absolute values of K_2 can be extracted from these data only if relative values of Φ_{complex} and Φ_{dye} are known (see below).

From the data of Table 1 complex formation appears somewhat, but not dramatically, solvent dependent. Statistically significant evidence for formation of ternary complexes is obtained (with one exception) only in methanol. From this result we cannot infer that 2 : 1 complexes do not form in the other solvents; they may form but not be fluorescence active. Statistically significant evidence of complexation between the dyes and **Im** was obtained only in methanol, where an effect akin to hydrophobic bonding [30,31] may be involved. This result is consistent with a hypothesis that ground state interaction involves π-complexation, as benzimidazole comprises a more extended π-electron system. Only in the non-hydrogen bonding solvents, acetone and acetonitrile, **I** is there evidence for complexation of dye **III** with **Bz**. (Ground state complexation of **III** may indeed occur under other conditions, but be transparent to the fluorescence probe). Fluorescence of dye **III** appears to be systematically quenched by **2-MeBz**, however.

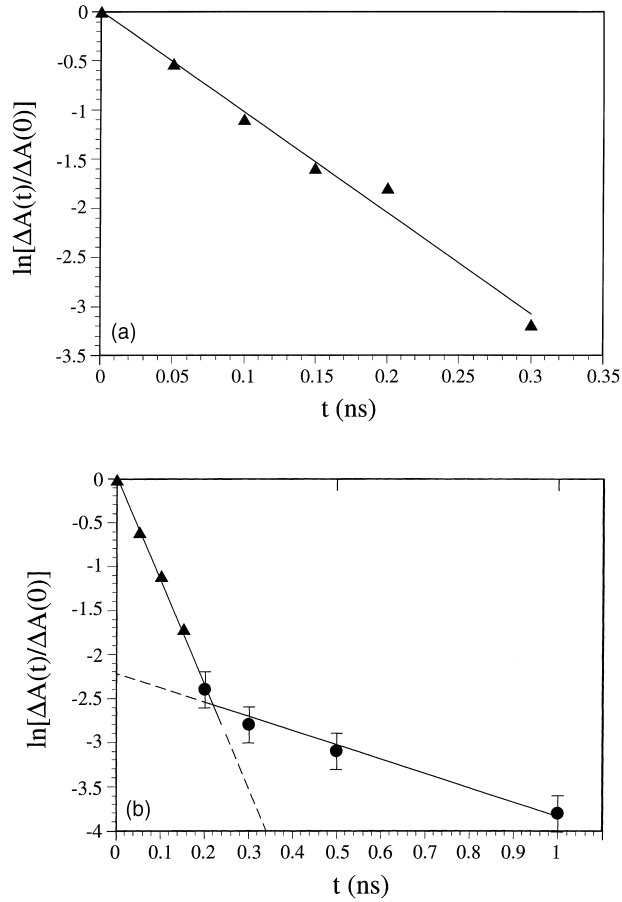

Fig. 4. Kinetics of recovery of optical absorption due to ground state dye **I** following laser flash excitation: (a) alone in methanol; (b) in the presence of 0.040 M **Bz** in methanol.

3.2. Time-resolved experiments

Lifetimes of the emissive S_1 states of dyes **I** and **II** alone and in the presence of 0.015 and 0.040 M **Bz** were measured in methanol by monitoring the recovery of ground state absorption following 30 ps laser flash excitation at 532 nm, using transient absorption spectroscopy. We expected that if our hypotheses of (a) formation of a 1 : 1 fluorescence-inactive complex, and (b) a 2 : 1 complex for which $\Phi_{\mathrm{complex}} > \Phi_{\mathrm{dye}}$, are correct, we should see biexponential recovery of dye ground sate. The shorter lifetime, τ_1, should be equal to the fluorescence lifetime of the dye alone. The longer component, τ_2, should be observable only in the presence of **Bz**. Both τ_1 and τ_2 should be independent of [**Bz**].

Representative transient absorption spectra obtained in experiments with both dyes **I** and **II** were shown in ref. [16]. Recovery of the ground state of **I** probed at 560 nm was treated according to pseudo-first order kinetics. Within the window of the experiment it was found to be singly exponential for the case of dye alone (Fig. 4(a)), but doubly exponential when **Bz** was present (Fig. 4(b)). The same situation obtained with dye **II**; recovery kinetics probed

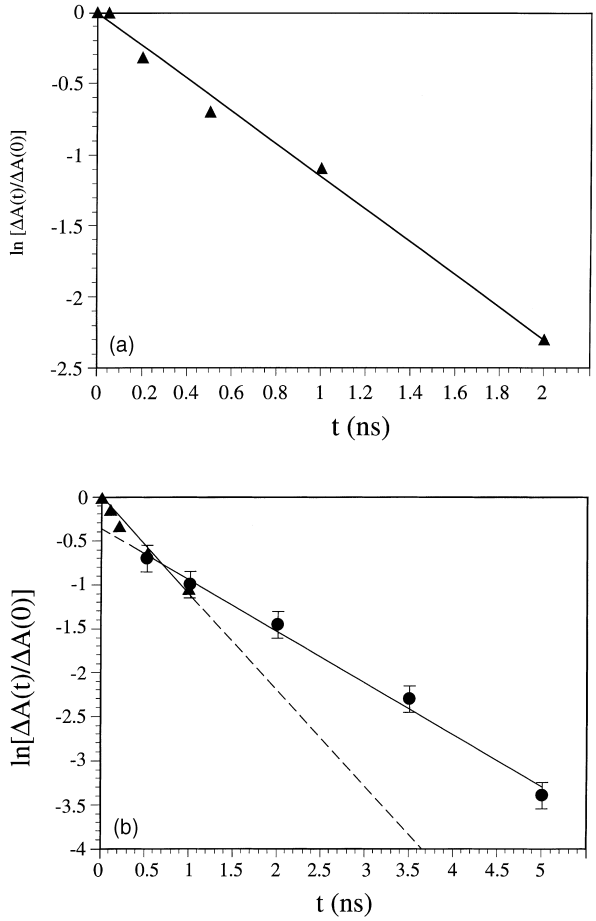

Fig. 5. Kinetics of recovery of optical absorption due to ground state dye **II** following laser flash excitation: (a) alone in methanol; (b) in the presence of 0.040 M **Bz** in methanol.

at 640 nm alone and in the presence of **Bz** are shown in Fig. 5(a–b), respectively. Lifetimes for the fast and slow components of the recovery, τ_1 and τ_2, respectively, for both dyes are given in Table 2. Variation in τ_1 was representative only of the inherent variability to be expected of the experimental technique. In all cases some bleaching of the ground state persisted beyond 5 ns. In our previous work [15,16] we attributed this observation to operation of the relaxation pathway leading to intersystem crossing and *trans–cis* isomerization of the chromophore. Values of $-\Delta A_\infty$, the residual bleaching of the ground state observable 5 ns after laser flash excitation, are also given in Table 2.

Table 2
Lifetimes for ground state recovery, dyes **I** and **II**, in methanol

Dye	[**Bz**] (M)	τ_1 (ns)	τ_2 (ns)	$-\Delta A_\infty$
I	0	0.10	–	0.06
	0.015	0.085	0.60	0.03
	0.040	0.14	0.67	0.04
	Average	(0.108 ± 0.023)	(0.635 ± 0.035)	–
	Literature (Ref. [16])	0.12	–	–
II	0	0.85	–	0.06
	0.015	0.75	1.50	0.05
	0.040	0.73	1.33	0.035
	Average	(0.78 ± 0.06)	(1.42 ± 0.08)	–
	Literature (Ref. [16])	0.64	–	–

From these data it is evident that fluorescence quenching of both dyes **I** and **II** cannot be explained by a dynamic mechanism, which would result in monotonically decreasing values of τ_1 with increasing [**Bz**]. Invariance of τ_1 with [**Bz**] confirms our hypotheses that ground state complex formation is responsible for fluorescence quenching and that the resulting complex is essentially fluorescence inactive. One possible mechanism for dissipating excitation energy in such a complex may be its dissociation [1], leading non-adiabatically to vibrationally excited dye and **Bz**.

Observation of a significant second decay component, τ_2, in the presence of **Bz** is consistent with the formation of a new, more fluorescent species when complexing agent is present. We assign this species, on the basis of Eq. (5) as the 2 : 1 benzimidazole : dye complex in both cases. From the relationship, $\Phi_{complex}/\Phi_{dye} = \tau_2/\tau_1$ implicit in this assignment, we can evaluate K_2 in these two cases. The estimates are included in Table 1.

The species responsible for τ_2 must also be a ground state complex. It is not conceivable for the 2 : 1 complex which we have assigned as the longer-lifetime, emissive species to form in the excited state by dynamic interaction of **Bz** with the excited, fluorescence-inactive complex, whose lifetime towards dissociation must be substantially less than the fluorescence lifetime of the dye itself. The 'dark' complex must dissipate the excitation energy on a time scale much shorter than τ_1, which accordingly does not allow it to live long enough to participate in any bimolecular reactions in solution.

Monotonic decrease in $-\Delta A_\infty$ with increasing [**Bz**] suggests that the rate limiting process for deactivation of the emissive complex does not lead to isomerization or intersystem crossing. These pathways are coupled to torsional relaxation in the excited free dye [7–16], and are responsible for the persistent bleaching observable at the longest delay times accessible in our experiments. On the contrary, we propose that complexation inhibits the prerequisite torsional relaxation of the excited dye.

3.3. Molecular recognition

Perturbation of fluorescence of dyes **I**, **II**, and **III** by the α,ω-bis(2-benzimidazolyl)alkanes was probed by titration in methanol. All the data could be fit to Eq. (1) or Eq. (5). Eq. (5) was used only when attempted fit of the experimental data to Eq. (1) failed to yield a coefficient of variation, $r^2 \geq 0.97$. Coefficients of variation for the two parameter fits were, in all cases, ≥0.98. We assume that the hypothesis developed to explain the applicability of Eq. (5) to the perturbation of the fluorescence of dyes **I** and **II** with **Bz** also applies here.

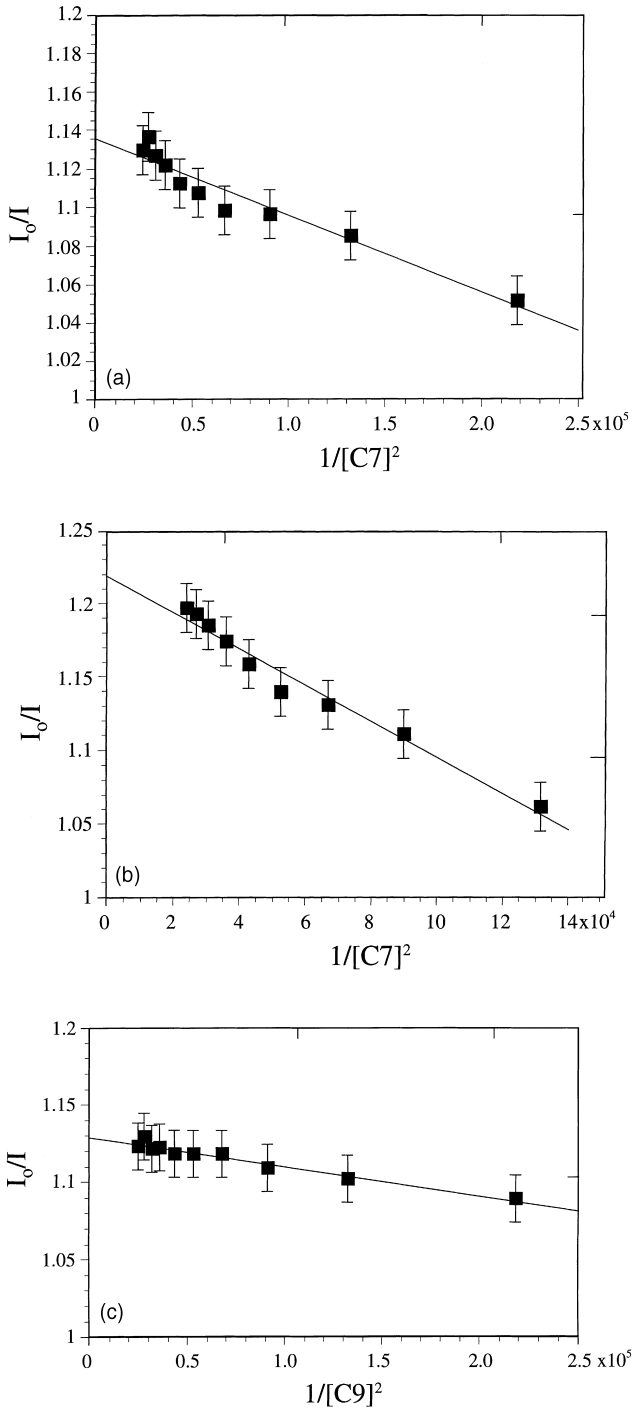

Fig. 6. Double reciprocal plots describing ternary complexation of: (a) dye **I** with $n = 7$ complexing agent; (b) dye **II** with $n = 7$ complexing agent; and (c) dye **II** with $n = 9$ complexing agent.

Where Eq. (5) was used a plot of I_o/I vs. $1/[Q]^2$ allows estimation of $\Phi_{complex}/\Phi_{dye}$. Accordingly, K_2 can be estimated directly from Eq. (A9). Double reciprocal plots, as I/I_o vs. $1/[Q]^2$ for the three cases requiring analysis according to Eq. (5) are shown in Fig. 6(a–c). These plots are linear over the concentration range, [Q], indicated, with $r^2 \geq 0.950$. On the other hand linear double reciprocal plots

Table 3
Parameters for complexation of cyanine dyes by α,ω-bis-(2-bemzimmidazolyl)alkanes of chain length *n*

Dye	*n*	K_1 (M^{-1})	$\Phi_{complex}/\Phi_{dye}$	K_2 (M^{-2})
I	3	14	–	–
	5	28	–	–
	7	31	1.13	1.6×10^4
	9	14	–	–
	11	23	–	–
II	3	23	–	–
	5	26	–	–
	7	42	1.23	1.08×10^4
	9	28	1.13	3.4×10^4
	11	20	–	–
III	3	15	–	–
	5	20	–	–
	7	16.5	–	–
	9	12	–	–
	11	10	–	–

were not obtained for other combinations of dye and complexing agent where Eq. (1) was applicable. Estimates of K_1 and K_2 are given in Table 3; confidence limits for both parameters are ca. ±25%. All the K_1 estimates for these complexing agents are substantially larger than observed with **Im** or **Bz**, in accord with the expectations from the computational chemical evaluation of the interaction of the dyes with the model complexing agent, **2-MeBz**; see below.

Estimates of K_1 for dye **I** are an order of magnitude too large to be accounted for by dynamic quenching. Contrary to our expectations from Scheme 1, however, these K_1 values reflect only a marginal level of molecular recognition, with maximum values of K_1 achieved where $(n-4)$ matches the number of methine carbon atoms in the cyanine dye. The complexing agents apparently express little or no significant selectivity in the strength of the complexes they form with dye **III**. With dye **I** there is evidence for formation of a ternary complex only where $n = 7$. Dye **II** forms ternary complexes with the $n = 7$ and 9 alkanes. There is no evidence of formation of a ternary complex between any of the alkanes and dye **III**. By inference from the results with dyes **I** and **II**, such a ternary complex might be expected with the $n = 11$ complexing agent. In summary, molecular recognition is observed, but primarily insofar as α,ω-bis(2-benzimidazolyl)alkanes of chain length *n* selectively enhance fluorescence of cyanine dyes when $(n-4)$ corresponds to the number of methine carbon atoms in the cyanine chromophore.

Additional perspective on the results in this series of experiments was provided by molecular mechanics (Merck molecular force field, MMFF) computations on the α,ω-bis(2-benzimidazolyl)alkanes. Minimum energy conformations for these complexing agents in solution are all twisted, folded structures, as illustrated for the minimum energy conformation of the $n = 7$ compound shown in Fig. 7. Calculated differences in strain energy, ΔG, between the folded and fully extended, open chain conformations are

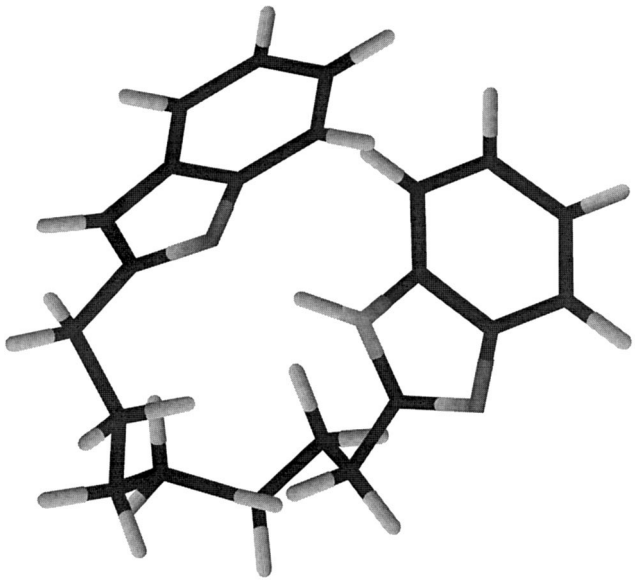

Fig. 7. Minimum energy conformation of $n = 7$ complexing agent, as derived using the Merck molecular force field (MMFF).

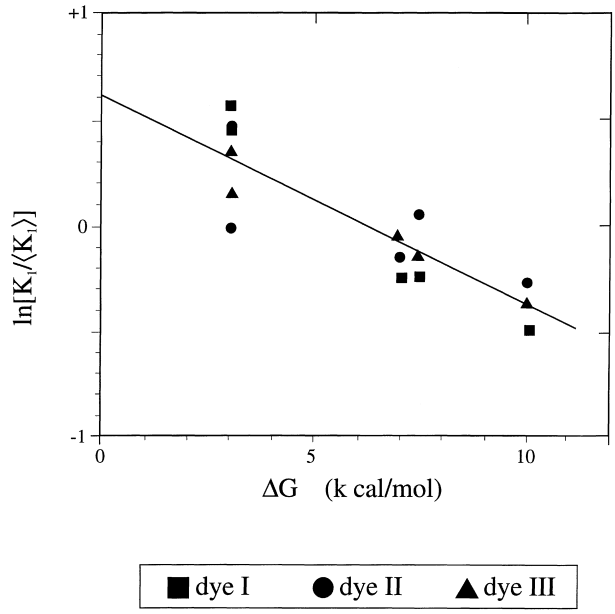

Fig. 8. Scatter graph for regression of normalized K_1 values, as $\ln(K_1/\langle K_1\rangle)$, on ΔG, the free energy for conversion of the equilibrium conformation, e.g., as shown in Fig. 7, of α,ω-bis-(2-bemzimidazolyl)alkane complexing agents to their corresponding chain extended forms.

given in Table 4. A scatter graph of $\ln(K_1/\langle K_1\rangle)$ vs. ΔG, where $\langle K_1\rangle$ is the average of K_1 values obtained with a given dye and all complexing agents of the same series, is shown in Fig. 8. The regression analysis is statistically significant ($r^2 = 0.734$), suggesting that unfolding of the complexing agent from its minimum energy conformation into its chain-extended form is prerequisite to complexation.

3.4. Computational studies on cyanine dyes and complexes

Computational chemical studies in the literature on cyanine dyes have largely been directed towards estimation of electronic transition energies, i.e., simulation of absorption spectra, ionization potentials and electron affinities, using relatively primitive computational procedures [32–34]. Some MINDO/pm3 calculations have been reported recently [35]. Molecular mechanics calculations have been used to predict geometries and, accordingly, spectral characteristics of H- and J-aggregates of some cyanine dyes [36].

Molecular mechanics calculations were carried out on the dyes **I**, **II** and **III**. The minimum energy form of dye **I** was found, using MMFF, to correspond to the *trans*-anti-isomer, in contrast to crystal structure determinations [37,38] which show that crystallization from solution leads exclusively to deposition of the *trans*-syn-isomer. It appears that in the gas phase (and, presumably, in solution) intramolecular dipole–dipole interactions stabilize the anti-conformation, while in the solid state intermolecular dipole–dipole interactions serve to stabilize the syn-conformation.

Table 4
Merck force field calculated strain energies for open chain vs. folded conformations of α,ω-bis-(2-bemzimidazolyl)alkanes

n	ΔG (kcal/mol)
3	7.12
5	3.01
7	3.02
9	7.31
11	10.08

For dye **II** energy minimization leads again to the anti conformation for the all-*trans* isomer, but only 0.26 kcal/mol below the syn conformation (neglecting any differences in solvation energy between the two isomers). Both structures might be expected to coexist in solution. In this case the two conformations of the all-*trans* isomer exhibit 3.33 and 2.57 kcal/mol less strain energy than their 8,9-*cis* counterpart. Photoisomerization of the all-*trans*-anti-isomer is expected [9] to lead to the 8,9-*cis*-syn isomer as the metastable photoproduct [39–41]. Optoaccoustic spectroscopy has indicated an energy difference between the *trans* and *cis*-photoisomers of dye **II** in the ground state as 3.5 kcal/mol [41] in good agreement with the calculations. We accordingly infer an adequate degree of reliability to the MMFF calculations for these dyes, consistent with the general experience in conformational optimization of organic molecular structures [27]. Accordingly MMFF provides a good account in most cases, while semi-empirical molecular orbital methods are, at best, not necessarily reliable. From the MMFF calculations we further infer that in solution, dye **III** is likely to be a mixture of an even greater number of equilibrating isomers, and solvation energy is likely to play a large role in determining which isomer(s) are dominant under given conditions.

With regard to the basis for complex formation, inspection of electrostatic charge distributions in the dye and

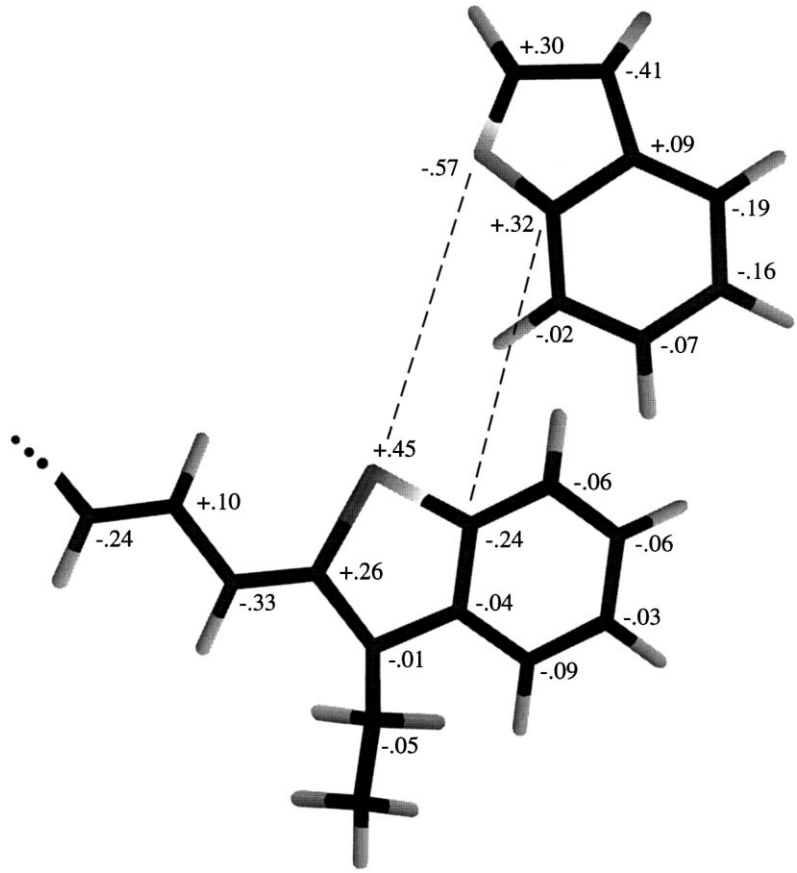

Fig. 9. Electrostatic charge distribution in half of the molecular structure of dye **II** and in the complexing agent **Bz**; dashed lines indicate axes of electrostatic attraction driving complex formation.

complexing agent molecules from the AM1 calculations proved especially informative. Surprisingly, in all of the dyes the sum the electrostatic charges associated with the atoms of the π-electron bearing framework was negative, despite the cationic character of the chromophores. This was a reflection of substantial delocalization of positive charge to the peripheral protons of the molecules, presumably involving hyper-conjugation. Hyper-conjugation is thought to be involved in the exchange mechanism of *cis–trans* photoisomerization in compounds such as stilbene and retinal [42]; a similar pathway is a principal route for excitation energy dissipation in cyanine dyes [8–11].

Fig. 9 shows the charge distribution for half of the structure of dye **II**, along with that for the complexing agent, **Bz**. Charge distributions in dyes **I** and **III** are similar to that of dye **II**. The charge distributions for all the dyes do not appear to be exactly symmetrical about the meso-carbon atom. Rather, the molecules are shown by the AM1 calculations to undergo Jahn–Teller distortion to C_1 symmetry to separate two otherwise degenerate HOMO states localized on the ring systems at opposite ends of the molecule. The representative HOMO surface for dye **I** is shown in Fig. 10. Those for dyes **II** and **III** are quite similar. It is quite different from the symmetrical, highly delocalized HOMO states inferred on the basis of simple Hückel molecular orbital calculations [32–34].

The search for minimum energy conformations of dye complexes was initially restricted, for reasons of practicality, to geometries in which the complexing agent, e.g., **Im** or **Bz**, is 'sandwiched' with one of the aromatic nuclei of the dye chromophore, i.e., π-complexation [43]. The gas phase enthalpy of formation of the complex from its individual components, ΔE, for any candidate geometry can then be approximated as [36]

$$\Delta E = \sum_i \sum_j (\boldsymbol{r}/4\pi\varepsilon)(q_i q_j / r_{ij}^2) - (A_{ij}/r_{ij}^6) + (B_{ij}/r_{ij}^{12}) \quad (6)$$

where q_i and q_j represent the individual electrostatic charges on atoms of the dye and complexing agent, respectively, where r_{ij} is the (scalar) interatomic spacing between each such pair of atoms, and $\boldsymbol{r}$ is the vector separation between the planes of the dye and complexing agent rings, taken at this point to correspond to the graphitic interlayer spacing, 3.4 Å. Since this value also corresponds to the sum of the van der Waals radii of the carbon atoms in the two ring systems, the second and third terms in Eq. (6), corresponding to attractive and repulsive dispersion forces,

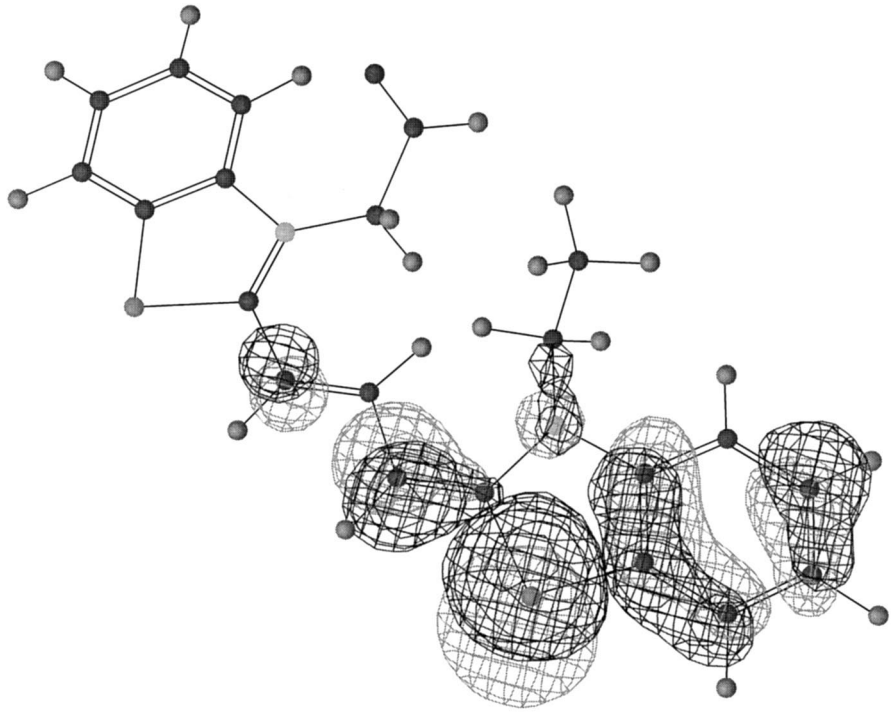

Fig. 10. HOMO surface for dye **I** from AM1 calculation.

respectively, cancel out [44], and only the first term need be evaluated.

Within the range of possible complex structures investigated here, we found that when the benzimidazole molecule is allowed to approach any of the dyes as shown in Fig. 9, with the trigonal nitrogen of the complexing agent approximately eclipsed with the ring sulfur atom of the dye, and the benzene rings of the complexing agent and dye superimposed $-\Delta E$ is maximized. Fig. 11 shows a section through the potential energy surface calculated according to Eq. (6) illustrating variation in ΔE with Θ, the angle between molecular axes of dye **I** and **Bz**, defined as shown in the figure. In this case we estimate a minimum in ΔE for $\Theta = (51 \pm 4)^\circ$.

The representative minimum energy structure for the complex of dye **I** with **Bz** based on AM1 calculation is shown in Fig. 12(a). Conformations in which the complexing agent is fully eclipsed with the heterocyclic ring system of the dye are again found to be repulsive. Similar structures were obtained for dyes **II** and **III**. Geometries of complexes with **2-MeBz**, chosen as a model of the α,ω-bis(2-benzimidazolyl)alkanes, were similar to those with **Bz**.

Quite different results were obtained from the AM1 calculations for the **Im** complexes, as illustrated by its complex with dye **I** in Fig. 12(b). In this case, the **Im** ring becomes centered over the carbon atom at the 2-position in the dye heterocyclic ring. Estimates of $-\Delta E$ for all dye-complexing agent combinations according to Eq. (6) are given in Table 5, part A. In the AM1 calculations we also found a small but significant tilt between the planes of the aromatic rings of the dye and complexing agents (3–7°) which was not taken into account in these calculations. Charge distributions for all three dyes in their all-*trans*-syn forms were used in these calculations. We envision ternary complex formation with dyes **I** and **II** as involving formation of a second, structurally analogous complex at the opposite end of the dye molecule.

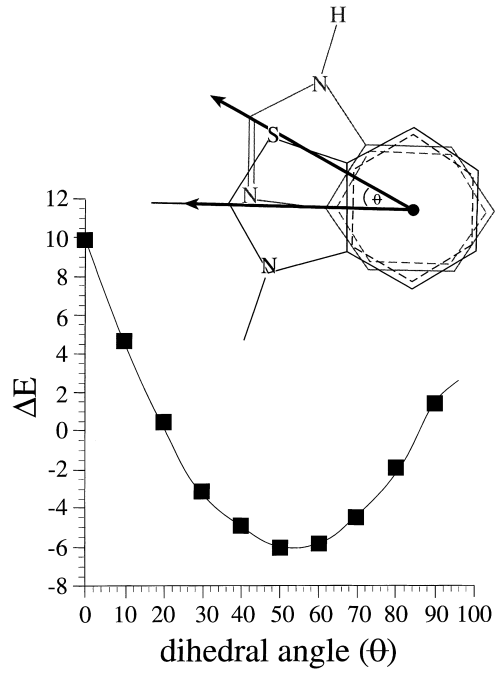

Fig. 11. Variation in ΔE estimated according to Eq. (6) with Θ, the angle between molecular axes of dye **I** and **Bz**, defined as shown in the inset.

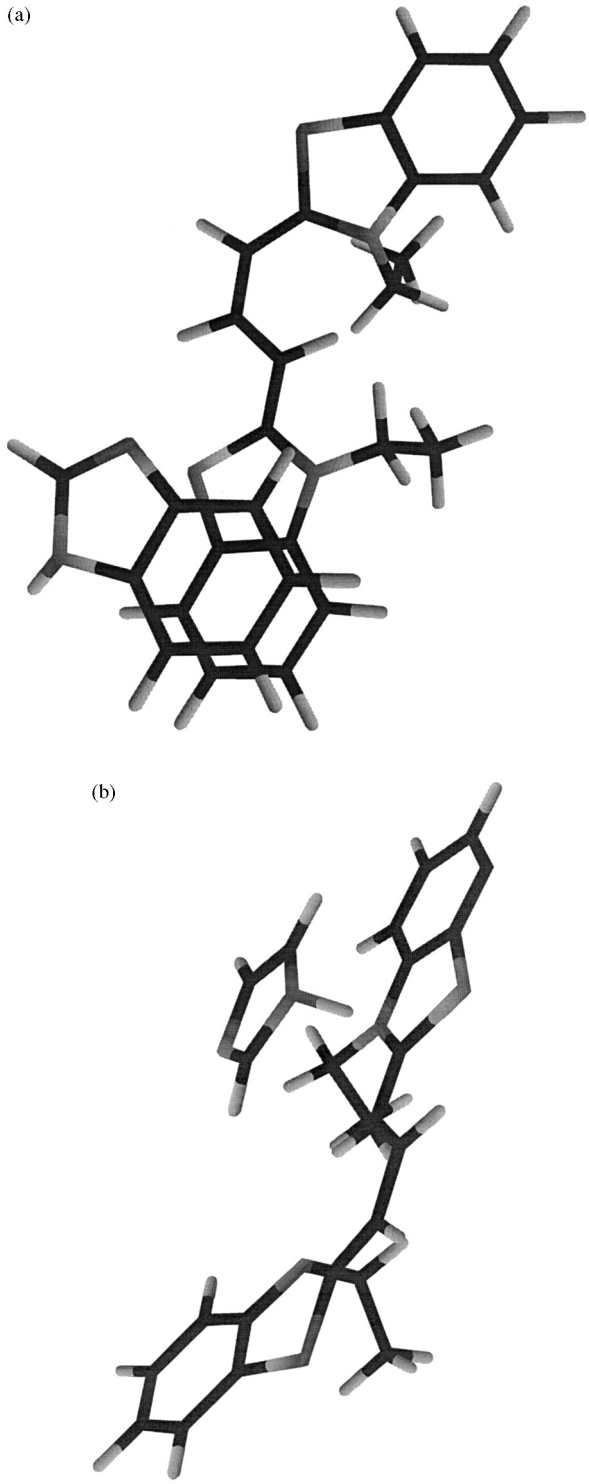

Fig. 12. Optimized geometry of the 1 : 1 complex formed between dye **I** in its syn-conformation and: (a) **Bz**; (b) **Im**.

In general, estimates derived from Eq. (6) suggest that **Im** complexes should be stronger than **Bz** complexes, and that dyes tend to form stronger complexes with increasing polymethine chain length. These expectations are not reflected in the pattern of the experimental data from Table 1. The estimates in Table 5 are, however, enthalpies,

Table 5
Estimates of gas phase enthalpies of complex formation, $-\Delta E$ (kcal mol^{-1})

Dye	**Im**	**Bz**	**2-MeBz**
A. From Eq. (6)			
I	9.5	5.8	9.8
II	10.9	9.2	20.5
III	15.7	15.6	24.4
B. From Eq. (7)			
I	21.5	7.2	17.3
II	12.6	4.4	12.2
III	18.2	11.5	21.3

while the data of Table 1 reflect free energy changes, which also include entropic contributions. Accordingly, dyes which initially posses more internal degrees of freedom may exhibit more negative entropy changes on complex formation than simpler, i.e., shorter chain, dyes. Estimates of gas phase binding energies furthermore completely neglect changes in solvation energy on complex formation, which may vary considerably among complexing agents.

The prediction of different geometries for **Im** and benzimidazole-derived complexes suggested that Eq. (6), as interpreted above, might not be an adequate approximation, however, and that dispersion forces could in fact play a significant role. Furthermore, estimates of $\boldsymbol{r}$, namely (3.1 ± 0.25) Å, shorter than the value assumed in parameterizing Eq. (6), resulted typically from geometry optimization in the AM1 calculations. An alternate approach [26–28] to estimation of $-\Delta E$ estimates heats of formation of dye, ΔH(dye), complexing agent, ΔH(complexing agent), and complex, ΔH(complex), by AM1 calculation. Then

$$\Delta E = \Delta H(\text{complex}) - [\Delta H(\text{dye}) + \Delta H(\text{complexing agent})] \quad (7)$$

with results as given in part B of Table 5. Estimates for $-\Delta E$ obtained by the two methods are, however, comparable, though the trend to stronger complexes with increasing polymethine chain length in the cyanine chromophore is not apparent in the data set of part B. We accordingly infer that the approximate evaluation of Eq. (6), in general, provides an adequately realistic description of the forces describing complex formation. Order of magnitude agreement between the estimates of $-\Delta E$ from Eqs. (6) and (7) for the complexes with **Im**, **Bz** and **2-MeBz** supports the assumption that complex formation is driven primarily by electrostatic forces, i.e., with little or no dispersion or charge transfer contributions. (Note, however, that the AM1 algorithm does not explicitly treat dispersion forces).

It is apparent that the geometry of the complexes as illustrated in Fig. 12(a) is incompatible with the rationale for molecular recognition proposed in Scheme 1. The geometry of the complex formed between dye **II** and 1,5-bis(2-benzimidazolyl)pentane, based on AM1 computation,

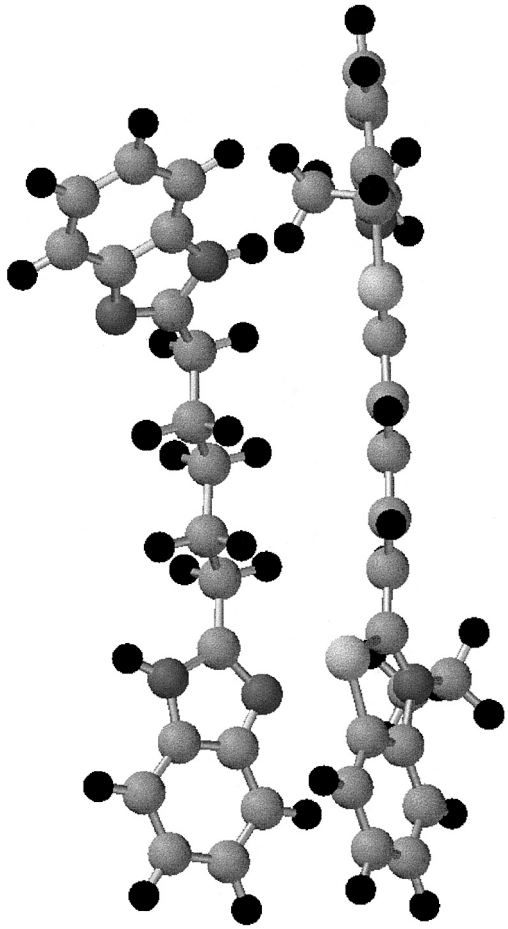

Fig. 13. Ball-and-stick representation of complex between dye **II** and 1,5-bis(2-benzimidizolyl)pentane ($n = 5$) based on AM1 calculation.

is shown in Fig. 13. The linear conformation of the complexing agent supports the inference, above, that linearization of the alkyl chain is prerequisite to complexation. The nearly perpendicular disposition of the aromatic heterocycles of the complexing agent relative to those of the dye is remarkably reminiscent of the geometry of the benzene dimer [45–48], in which association is driven, in part, by hydrogen bonding [48]. This arrangement of paired aromatic molecules is believed to be rather common in biological environments, as well [49].

4. Conclusions

Complexes between cyanine dyes, **I**, **II** and **III**, and **Im**, **Bz**, and **2-MeBz**, have been detected by perturbation of the dyes' fluorescence. In some cases 1 : 2, as well as 1 : 1 complexes, can be observed. This assignment has been confirmed by time-resolved laser flash spectroscopy, with recovery of the ground state of the dye detected by transient absorption spectroscopy. Based on a preconception concerning complex geometry, we selected a series of α,ω-bis(2-benzimidazolyl)alkanes of chain length n, as complexing agents which we anticipated might exhibit molecular recognition towards the cyanine chromophores. A modicum of molecular recognition was indeed observed when $(n-4)$ matched the number of carbon atoms in the polymethine chain of the dye.

Computational chemical studies using MMFF and AM1 semi-empirical molecular orbital calculation were carried out to identify complex structures. Geometry of the **Im** and **Bz**, as well as with the complexing agent **2-MeBz**, taken as a model of the α,ω-bis(2-benzimidazolyl)alkanes, turned out to be quite different, and the geometry of the latter complexes turned out to be incompatible with the anticipated basis for molecular recognition. The computational studies showed the basis for dye–complexing agent interaction in the ground state to be principally electrostatic, i.e., with little or no dispersion or charge transfer contributions.

Acknowledgements

Funding for this work was provided by the Imation Corp. Oakdale, MN, and by the Natural Sciences and Engineering Research Council of Canada (grant to Prof. N. Serpone, Concordia University). We thank Prof. Serpone for his generous hospitality at Concordia University, Montréal, Québec, where time-resolved experiments were carried out; we also thank Mr. Reza Danesh for his expert technical assistance with these experiments. We thank Dr. Ramaiah Muthyala, 3M Co., for guidance on the synthesis of the α,ω-bis(2-benzimidazolyl)alkanes, and Mr. J.R. Hill, 3M Corporate Research, for the 400 MHz proton NMR spectroscopy on our materials. Prof. L.O. Ochrymowycz (UWEC) provided helpful assistance with TLC characterization of the dyes. We thank Prof. Warren Gallegher (UWEC) for helpful guidance on the use of SPARTAN. The spectrofluorimeter used in these studies was a gift of the 3M Company to the University of Wisconsin – Eau Claire.

Appendix A

Consider the case of a dye, D, which can form two complexes with the complexing agent, Q, of stoichiometry Q : D and 2Q : D. The equilibrium constants for formation of these complexes are defined as follows:

$$K_1 = [\mathrm{Q} : \mathrm{D}]/[\mathrm{Q}][\mathrm{D}] \tag{A1}$$

$$K_2 = [2\mathrm{Q} : \mathrm{D}]/[\mathrm{Q}]^2[\mathrm{D}] \tag{A2}$$

and the fractional conversions of the dye population, for the case, $[\mathrm{Q}] \gg [\mathrm{D}]$, to the 1 : 1 and 2 : 1 complexes, f_1 and f_2, respectively are expressed by

$$f_1 = \left\{1 + (K_1[\mathrm{Q}])^{-1}\right\}^{-1} \tag{A3}$$

$$f_2 = \left\{1 + \left(K_2[\mathrm{Q}]^2\right)^{-1}\right\}^{-1} \tag{A4}$$

For relatively small degrees of complexation ($f \leq 0.1$), $K_1[Q]$ and $K_2[Q]^2 < 1$, so that these expressions simplify approximately to

$$f_1 = K_1[Q] \tag{A5}$$

$$f_2 = K_2[Q]^2 \tag{A6}$$

If we assume that the 1 : 1 complex is fluorescence inactive, but that the 2 : 1 complex is emissive with fluorescence quantum efficiency, $\Phi_{complex}$, then we can write the overall observed fluorescence quantum efficiency as

$$\Phi_{obs} = [1 - (f_1 + f_2)]\Phi_{dye} + f_2\Phi_{complex} \tag{A7}$$

Substitution of Eq. (A5) and Eq. (A6) into Eq. (A7) yields

$$\Phi_{obs} = \left[1 - \left(K_1[Q] + K_2[Q]^2\right)\right]\Phi_{dye} + K_2[Q]^2\Phi_{complex} \tag{A8}$$

which rearranges to

$$\Phi_{obs}/\Phi_{dye} = 1 - K_1[Q] + \left(\Phi_{complex}/\Phi_{dye} - 1\right)K_2[Q]^2 \tag{A9}$$

which is identical in form to empirical Eq. (5).

References

[1] M.R.V. Sahyun, J.T. Blair, J. Photochem. Photobiol. A Chem. 104 (1997) 179.
[2] H.-C. Becker, A. Broo, B. Nordén, J. Phys. Chem. A 101 (1997) 8853.
[3] T.L. Netzel, K. Nafsi, M. Zhao, J.R. Lenhard, I. Johnson, J. Phys. Chem. 99 (1995) 17936.
[4] S.C. Benson, P. Singh, A.N. Glazer, Nucleic Acids Res. 21 (1993) 5727.
[5] L.G. Lee, C.-H. Chen, L.A. Chiu, Cytometry 7 (1986) 508.
[6] H.S. Rye, S. Yue, D.E. Wemmer, M.A. Quesada, R.P. Haugland, R.A. Mathies, A.N. Glazer, Nucleic Acids Res. 20 (1992) 2803.
[7] D. Fassler, M. Baezold, J. Photochem. Photobiol. A Chem. 64 (1992) 359.
[8] S.H. Ehrlich, J. Phys. Chem. 79 (1975) 2228, 2234.
[9] F. Mommichioli, I. Baraldi, G. Berthier, Chem. Phys. 123 (1988) 103.
[10] G. Ponterini, F. Mommichioli, Chem. Phys. 151 (1991) 111.
[11] G. Ponterini, M. Casellli, Ber. Bunsenges. Phys. Chem. 96 (1992) 564.
[12] W. West, S. Pearce, F. Grum, J. Phys. Chem. 71 (1967) 1316.
[13] P.J. McCartin, ibid. 47 (1965) 2980.
[14] Yu.I. Lifanov, V.A. Kuz'min, A.K. Chibisov, I.I. Levkoev, A.V. Karyakin, Zh. Priklad. Spektrosk. 20 (1974) 221.
[15] N. Serpone, M.R.V. Sahyun, J. Phys. Chem. 98 (1994) 734.
[16] M.R.V. Sahyun, N. Serpone, ibid. 101 (1997) 9877.
[17] S.A. Soper, Q.A. Mattingly, J. Am. Chem. Soc. 116 (1994) 3744.
[18] G.M. Whitesides, E.E. Simanek, J.P. Mathias, C.T. Seto, D.N. Chin, M. Mammen, D.M. Gordon, Acc Chem. Res. 28 (1995) 37.
[19] D.G. O'Sullivan, D. Pantic, A.K. Willis, J. Med. Chem. 15 (1972) 103.
[20] W.R. Roderick, C.W. Nordeen, ibid. 15 (1972) 655.
[21] P.N. Preston, Chem. Rev. 74 (1974) 310.
[22] J.C. Lockhart, D.J. Rushton, J. Chem. Soc., Dalton Trans. (1991) 2633.
[23] P.C. Vas, C.K. Oza, A.K. Goyal, Chem. Ind. (1980) 287.
[24] P.T. Kissinger, W.R. Heineman, Laboratory Techniques in Electroanalytical Chemistry, Chap. 5, Marcel Dekker, New York, 1984.
[25] J.R. Lenhard, J. Imaging Sci. 30 (1986) 27.
[26] W.J. Hehre, SPARTAN, Version 4.0, Wavefunction, Inc., Monterey Park, CA, 1995.
[27] W.J. Hehre, J. Yu, P.E. Klunzinger, A Guide to Molecular Mechanics and Molecular Orbital Calculations in SPARTAN, Wavefunction, Inc., Irvine, CA, 1997.
[28] W.J. Hehre, W.W. Huang, P.E. Klunzinger, B.J. Deppmeier, A.J. Driessen, A SPARTAN Tutorial, Wavefunction, Inc., Irvine, CA, 1997.
[29] N. Serpone, D.K. Sharma, J. Moser, M. Grätzel, Chem. Phys. Lett. 136 (1987) 47 and references cited therein.
[30] W. Kauzmann, Adv. Protein Chem. 14 (1959) 1.
[31] C. Hansch, H. Kiehs, G.L. Lawrence, J. Am. Chem. Soc. 87 (1965) 5770.
[32] T. Tani, Photogr. Sci. Eng. 16 (1972) 258.
[33] D.M. Sturmer, W.S. Gaugh, Photogr. Sci. Eng. 16 (1972) 146.
[34] T. Tani, Photographic Sensitivity, Chap. 5, Oxford University Press, Oxford, UK, 1996.
[35] J.R. Lenhard, A.D. Cameron, J. Phys. Chem. 97 (1993) 4916.
[36] R.L. Parton, H.J. Price, I.A. Watson, in: S.C. Busman (Ed.), Advance Printing of Paper Summaries, IS&T's 44th Annual Conference, IS&T, Springfield, VA, 1991, 58 pp. (Eq. (6) in the present paper differs slightly from the version used by these authors, insofar as the Coulomb's law term in Eq. (6) is formulated to correspond to standard usage, e.g., H.C. Anderson, Physics Vade Mecum, American Institute for Physics, New York, 1981, 33 pp.).
[37] H. Nakatsui, Y. Hishiki, Photogr. Sci. Eng. 20 (1976) 68.
[38] P.J. Wheatley, J. Chem. Soc. (1959) 3255, 4096.
[39] A.K. Chibisov, H. Görner, J. Photochem. Photobiol. A Chem. 105 (1997) 261.
[40] V. Khimenko, A.K. Chibisov, H. Görner, J. Phys. Chem. A 101 (1997) 7304, and references cited therein.
[41] G.M. Bilmes, J.O. Tocho, S.E. Braslavsky, J. Phys. Chem. 93 (1989) 6696.
[42] V. Deckert, K. Iwata, H. Hamaguchi, J. Photochem. Photobiol. A Chem. 102 (1996) 35.
[43] Operationally this constraint is achieved in the SPARTAN algorithm by tethering the dye and complexing agent heterocyclic ring systems together with flexible, typically three-carbon alkane chains for a preliminary geometry minimization. The chains can then be removed for the actual MMFF and AM1 calculations. See Ref. [28].
[44] J.N. Murrell, S.F.A. Kettle, J.M. Tedder, The Chemical Bond, 2nd ed., Wiley, Chichester, UK, 1985, 295 pp.
[45] K.C. Janda, J.C. Hemminger, J.S. Winn, S.E. Novick, S.J. Harris, W. Klemperer, J. Chem. Phys. 63 (1975) 1419.
[46] P. Hobza, H.L. Selzle, E.W. Schlag, Chem. Rev. 94 (1994) 1767.
[47] P. Hobza, H.L. Selzle, E.W. Schlag, J. Phys. Chem. 100 (1996) 18790.
[48] P. Hobza, V. Spirko, H.L. Selzle, E.W. Schlag, J. Phys. Chem. A 102 (1998) 2501.
[49] C.A. Hunter, J. Singh, J.M. Thornton, J. Mol. Biol. 218 (1991) 837.